Commun Nonlinear Sci Numer Simulat 16 (2011) 4558–4563

Contents lists available at ScienceDirect

Commun Nonlinear Sci Numer Simulat

journal homepage: www.elsevier.com/locate/cnsns

Pinning and mode-locking of reaction fronts by vortices

Garrett M. O'Malley, Matthew S. Paoletti [1], Mollie E. Schwartz [2], Thomas H. Solomon *

Department of Physics and Astronomy, Bucknell University, Lewisburg, PA 17837, USA

ARTICLE INFO

Article history:
Available online 13 May 2011

Keywords:
Chaotic behavior
Advection–reaction–diffusion
Front propagation
Mode-locking
Vortices

ABSTRACT

We present results of experiments on the behavior of reaction fronts in the presence of vortex-dominated flows. The flow is either a single vortex or a chain of vortices in an annular configuration, and the reaction is the excitable Belousov–Zhabotinsky chemical reaction. If the vortex chain oscillates periodically in the lateral direction, the reaction front often mode-locks to the oscillations, propagating an integer number of wavelengths of the flow (two vortices) in an integer number of drive periods. In the presence of a uniform "wind", the front often freezes, remaining pinned to the leading vortex and neither propagating forward against the wind nor being blown backward by it. Studies with an individual vortex verify the ability of a moving vortex to pin and drag a reaction front. We use this pinning behavior to explain the mode-locking for the oscillating case.

1. Introduction

There is significant interest in the behavior of reaction fronts in a fluid system [1,22], a problem with applications in many fields of science and engineering [9,10,14,15]. In the *reaction–diffusion* (RD) limit with no fluid flows, the speed at which a reaction front propagates was predicted in the 1930's to be given by the Fisher–Kolmogorov–Petrovskii–Piskunov (FKPP) result $v = \sqrt{2Dk}$ where D and k are the molecular diffusivity and reaction rates of the relevant species involved in the reaction [7,11]. The effects of fluid flows on front behavior, however, is still not understood, even for well-ordered, laminar flows. In many cases, transport in a fluid flow is diffusive in nature with the variance of a distribution that grows as $\langle \sigma^2 \rangle = 2D^* t$ where D^* is the enhanced diffusivity. It is natural in these cases to assume that the FKPP prediction still holds but with D replaced by D^*. In fact, this result seems almost so obvious that many investigators overlook this problem and instead concentrate on extensions of FKPP theory to cases where the transport is superdiffusive with $\langle \sigma^2 \rangle \sim t^\gamma$ with $\gamma > 1$ [3,5,12].

In this paper, we present experiments that demonstrate that FKPP theory does not adequately describe front propagation in laminar flows, even in situations where the transport is diffusive. Instead, front propagation is dominated by the presence of coherent vortices in the flow that tend to pin and drag fronts. Coherent vortices are prevalent in a wide range of flows, including turbulent flows such as the Great Red Spot of Jupiter [13,21]; consequently, the role of vortices is important for a wide range of systems.

In Section 2, we describe the experimental apparatus and flow, along with the chemistry used to produce the fronts. In Section 3, we describe experiments that show mode-locking in front propagation with periodic time dependence. Pinning of reaction fronts by vortices is described in Section 4. We discuss areas for future study in Section 5.

* Corresponding author.
E-mail address: tsolomon@bucknell.edu (T.H. Solomon).
[1] Current address: Department of Physics, University of Maryland, College Park, MD 20742, USA.
[2] Current address: Science and Technology Policy Institute, Washington, DC 20006, USA.

1007-5704/$ - see front matter © 2011 Elsevier B.V. All rights reserved.
doi:10.1016/j.cnsns.2011.05.008

2. Experimental techniques

The flow is either a single vortex or a chain of 20 vortices in an annular configuration [16–20]. The flow is driven using a magnetohydrodynamic technique, as shown in Fig. 1. An electrical current passes radially through a thin (2 mm) layer of an electrolytic solution, interacting with a varying magnetic field produced by two rings of alternating magnets below the fluid layer. The result is a flow with 20 vortices within the annulus. The magnet assembly is mounted on a motor; the magnet assembly and the magnets rotate with the motor, causing lateral motion of the vortices within the flow. If the motor oscillates, then the vortices oscillate. If the motor moves with a constant angular velocity, then the vortices drift around the annulus with a constant speed. A combination of oscillation and drift is also used. Throughout this paper, the magnitude of the oscillations is denoted by the maximum lateral oscillation speed v_o, and the drift speed is denoted by v_d. Previous studies [19] have shown that long range transport is typically diffusive if $v_o > v_d$ and is typically superdiffusive if $v_o < v_d$. With this experimental approach, therefore, we are able to switch between diffusive and superdiffusive transport.

The working fluid is composed of the chemicals used for the excitable Belousov–Zhabotinsky chemical reaction [6,8,2,17,18,20]. We use the Ruthenium-catalyzed BZ reaction, which is photosensitive. An LCD projector shines a template image on the apparatus, with red light over the annular region and blue-green light everywhere else. The reaction is inhibited by the blue-green light but not the red light. This approach prevents spurious reaction fronts from entering the region of interest. The reaction itself is triggered by inserting a silver wire into the flow. This causes the Ruthenium indicator (which is initially orange) to oxidize, turning green. The oxidized Ruthenium triggers the surrounding regions, resulting in a reaction front that propagates outward from the trigger source. When the radial current is applied, vortices form in the annulus and the reaction is also advected with the fluid flow. The resulting advection–reaction–diffusion process is imaged from above with a high-resolution CCD camera with an orange filter. All of the images shown in this paper are "de-curled" – digitally cut and unwrapped so that they can be displayed as horizontal strips.

3. Mode-locking

If the vortex chain oscillates periodically in the lateral direction (with no drift: $v_d = 0$), the front often mode-locks to the external forcing, traveling an integer number N of wavelengths of the flow (where one wavelength is two vortex widths) in an integer number M of drive periods [4,17,18]. An example of mode-locking with combination $(N,M) = (1,1)$ is shown in Fig. 2, along with a simulation [18] of similar (1,1) mode-locking. The front can be seen to move precisely two vortices (one wavelength) each drive period, consistent with the definition of mode-locking for front propagation.

Quantitatively, mode-locking is associated with a front speed $v = N\lambda/MT = (N/M)\lambda f$. We measure the front velocities to determine if the front is mode-locked and, if so, what combination of N and M describes the locking. Fig. 3(a) shows the experimental front velocities for the pure oscillatory case along with the predictions based on mode-locking. A parameter-space diagram (Fig. 3(b)) shows regions of non-dimensional amplitude and frequency of oscillation for which there is (1,1) and (1,2) mode-locking. (There is an overlap region as well, where the front alternates speed between the two (1,1) and (1,2) speeds).

These results are clearly inconsistent with an FKPP approach. According to the FKPP prediction, the front velocity should grow with effective diffusivity D^*. Some of the lower-frequency cases have front velocities that are smaller than the case with no oscillations at all [18], despite the fact that any oscillating case (i.e., $v_o \neq 0$) has an effective diffusivity significantly higher than the non-oscillating case. Furthermore, the dramatic changes in propagation velocity when the front switches from one mode-locked regime to another (or becomes unlocked) cannot be explained by the FKPP theory.

4. Pinning of reaction fronts

If the vortex chain drifts with a constant angular velocity ($v_o = 0$, $v_d \neq 0$), there is a strong tendency for the front to pin to the vortex chain [20]. Fig. 4 shows sequences of images for different drift speeds. The images are all shown from the refer-

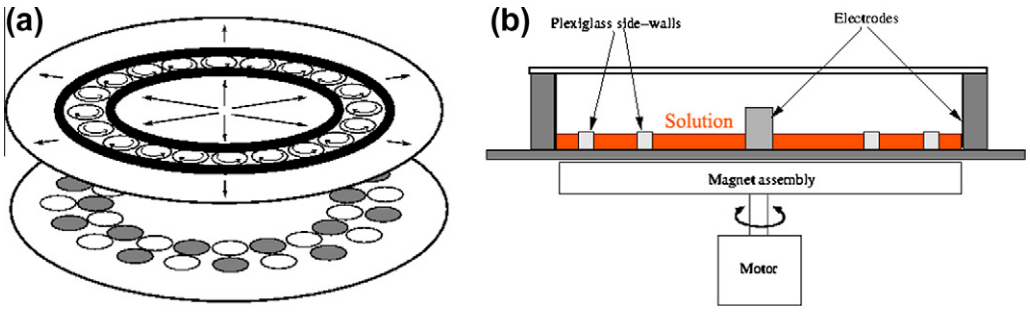

Fig. 1. Apparatus used to generate annular chain of vortices. (a) Exploded view of magnetohydrodynamic, showing radial current, magnets below the fluid layer, and vortex chain within the annulus. (b) Side view of apparatus.

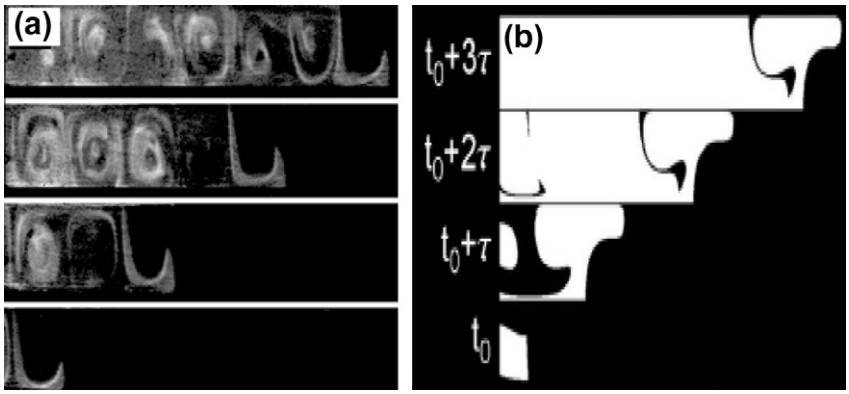

Fig. 2. Sequences showing (1,1) mode-locking where the front propagates 1 wavelength (2 vortex widths) each drive period. The vortex chain oscillates periodically with no drift ($v_d = 0$). (a) Experimental sequence; each image separated in time by one period. (b) Numerical simulation.

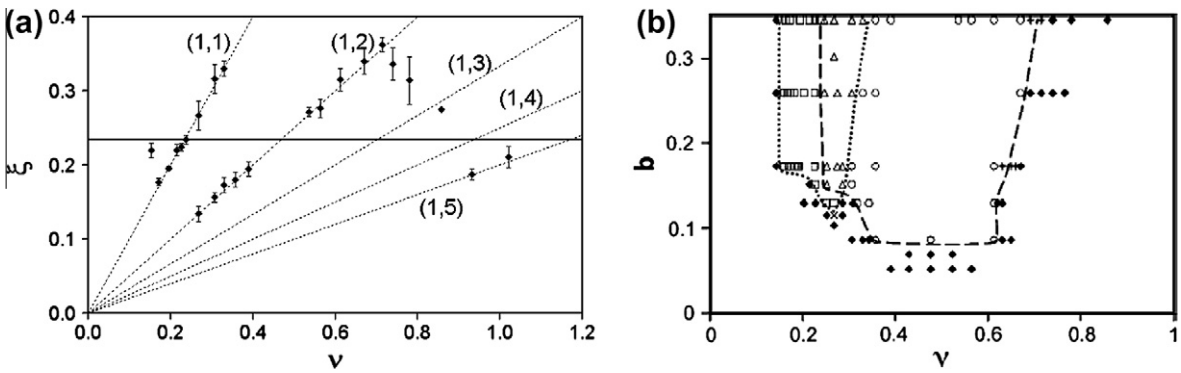

Fig. 3. (a) Experimental results showing non-dimensional front speed ξ as a function of non-dimensional frequency ν. The dotted lines show the theoretical predictions for mode-locked speeds. (b) Parameter-space plot showing regimes for (1,1) and (1,2) mode-locking. Filled diamonds denote unlocked states, whereas open squares, open circles and open triangles denote states with (1,1), (1,2) and combination (1,1)/(1,2) mode-locking, respectively.

ence frame of the moving vortices; in this frame, the vortices appear stationary and there is an imposed, uniform "wind" with a wind speed v_d. For small drift/wind speeds (Fig. 4(a)), the front still manages to propagate against the wind. For a large range of drift/wind speeds, the front is frozen with respect to the vortex chain, as shown in Fig. 4(b). If the drift/wind is sufficiently large, the front is "blown" backward, as shown in Fig. 4(c). This behavior does not depend on whether or not the vortices are in an ordered or disordered pattern; as seen in Fig. 4(d), reaction fronts are pinned in the face of an opposing wind even for disordered vortex flows.

Different types of front behavior are possible if there is *both* drifting and oscillation of the vortex chain. Of course, frozen (pinned) fronts are possible, as well as mode-locked fronts. There is also a "Sisyphus" state in which the front momentarily propagates forward against the wind but is then blown backward when the lateral oscillation is in the same direction as the drifting. The net result of the Sisyphus state is a front that remains stationary overall.

An important question is the dependence of the front behavior on the type of transport in the system. In these experiments, the long-range transport changes from diffusive to superdiffusive when the drift velocity v_d is increased beyond the maximum oscillatory velocity v_o. A parameter-space diagram (Fig. 5) shows that mode-locking behavior drops out when v_d exceeds v_o, coincident with the transport becoming superdiffusive. There are other things that change about the flow at the $v_d = v_o$ line, so the drop-out of mode-locking is not necessarily due specifically to the change in transport from diffusive to superdiffusive. For instance, there is a wavy jet that weaves between the vortices that is periodically cut when $v_d < v_o$ but which remains intact when $v_d > v_o$. Furthermore, front propagation in cases with diffusive mixing is not always characterized by mode-locking. Consequently, it is not possible at this point to use this data to test current theories about the effects of superdiffusion on front propagation [12,5,3]. Additional research is needed to address more generally the differences in front propagation between cases with diffusive and superdiffusive transport.

A simple modification to the experimental apparatus in Fig. 1 enables us to generate a flow with a single vortex instead of a vortex chain. Instead of having two rings of magnets in the magnet assembly below the fluid, we place only two magnets (with opposite polarity) on the plexiglass disk attached to the motor. Experimentally, we turn on the radial current, trigger a reaction front at some location in the annulus, allow the front to propagate outward until it spans the annular region, and

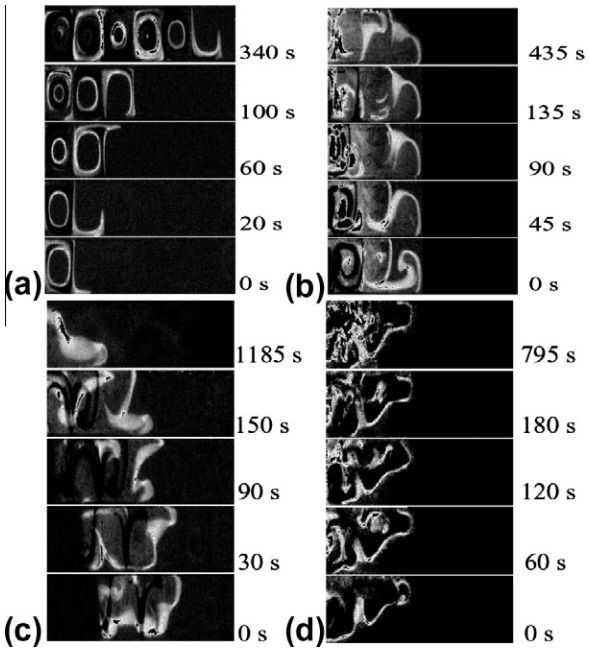

Fig. 4. Experimental sequences showing front propagation in the presence of an opposing, uniform wind blowing right-to-left. (a) Small wind; front propagates forward to the right. (b) Intermediate wind; front is frozen in the leading vortex. (c) Strong wind; front is blown back to the left by the wind. (d) Sequence with random vortex flow; the front still freezes.

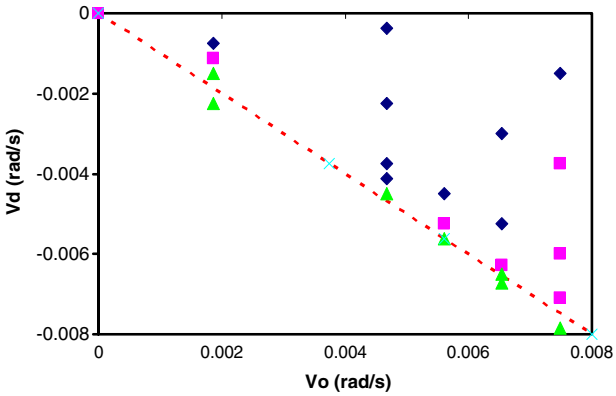

Fig. 5. Parameter-space diagram showing drop-out of mode-locking when drift exceeds oscillation of vortex chain. Diamonds correspond locked fronts, squares partially-locked, and triangles unlocked. The dashed line corresponds to the condition $v_d = v_o$, where the transport changes from diffusive to superdiffusive.

then start the motor. The fluid in the annulus above the magnet pair has a vortex which moves around the annulus above the two magnets. When the magnet pair passes below the region with the reaction front, the vortex itself passes through the reaction.

Fig. 6 shows spacetime plots corresponding to the collision of a single vortex with a reaction front. The dark lines in Fig. 6 show the leading edges of the reaction front, and the moving vortex – which is moving to the left in these sequences – can be seen as a diagonal white line. For early times, the reaction front (initiated near the right in both Figs. 6(a) and (b)) moves slowly in both directions (seen by the large slopes at early times) since there is no flow in the vicinity. When the vortex reaches the reaction front, there is a small deflection of the right-ward moving front, but the vortex mainly passes through, as is always the case when the vortex and front are propagating in opposite directions. The left-ward moving vortex grabs the left-ward moving front. If the vortex is traveling too fast (Fig. 6(a)), the front drops off after a few moments. On the other hand, if the vortex is moving slightly slower (Fig. 6(b)), it pins and drags the front for the duration of the experiment.

Fig. 7 shows a parameter-space diagram that characterizes the conditions in which a moving vortex pins and drags a reaction front indefinitely. The horizontal axes denotes the non-dimensional speed ε at which the vortex is moving, normalized

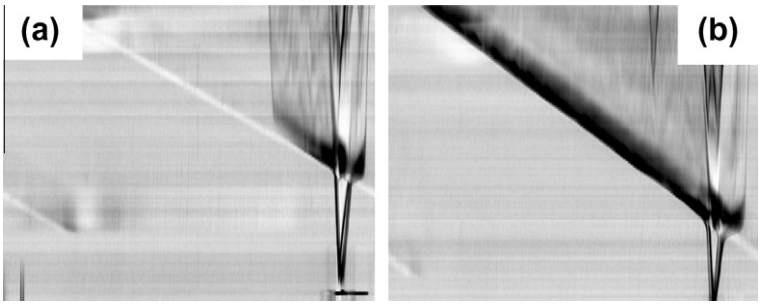

Fig. 6. Spacetime plots (with time increasing along vertical) showing interaction between a reaction front and a moving vortex. (a) Fast-moving vortex temporarily drags front, but pinning drops out as vortex (white diagonal line) continues onward. (b) Slightly slower vortex pins and drags reaction front indefinitely.

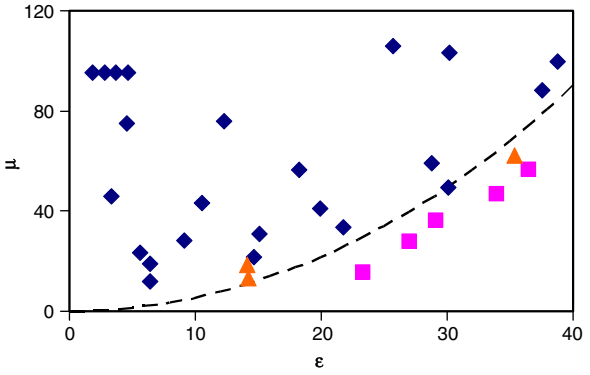

Fig. 7. Parameter-space diagram showing pinning of reaction front by moving vortices. The non-dimensional vortex strength μ is the maximum flow velocity within the vortex, normalized by the reaction–diffusion front propagation speed v_{rd}. The non-dimensional lateral speed ε of the vortex is the vortex speed divided by v_{rd}. The diamonds/squares/triangles denote pinned fronts, unpinned, and marginally-pinned fronts, respectively. The dashed curve denotes an approximate boundary between pinned and unpinned states.

by the speed at which a front propagates in the reaction–diffusion regime (with no fluid flows). The vertical axis denotes the non-dimensional vortex strength μ, defined as the maximum vortex velocity divided by the RD speed.

We can now explain the mode-locking discussed in Section 3 in terms of the pinning of the reaction front by moving vortices. If the vortex chain is oscillating periodically in the lateral direction, then during half of the period, the vortices are moving in the same direction as the front. During the other half, the vortices are moving against the reaction front. When moving in the same direction as the front, the vortices pin and drag the front with them (if v_o is large enough). When the vortices reverse direction, they release the reaction front since there is no pinning when the vortices travel in a direction opposite that of the fronts. The process repeats with the same period as the vortex oscillation, with the front being dragged by the vortices when they move one direction, and then being released when the vortices move the opposite direction. This provides a "ratcheting" mechanism by which the front motion is locked to the frequency of oscillation.

5. Discussion

Ultimately, a general theory is needed to describe front propagation in advection–reaction–diffusion systems. In flows dominated by moving vortices, it might be possible to use front pinning to describe front motion. With this approach, the velocity field can be replaced by a collection of point vortices, with each vortex assigned a strength based on the circulation determined from the velocity field. The effect on front propagation of each vortex moving through the system can then be determined to first-order by the parameter-space diagram of Fig. 7. If a vortex collides with the front, moving in the same direction as the front, then that vortex pins and drags the front if its circulation and lateral speed are within the pinning range of Fig. 7.

Experiments are currently under way to test the applicability of a pinning-centered approach to describing front propagation in a complicated vortex-dominated flow.

References

[1] Abel M, Celani A, Vergni D, Vulpiani A. Front propagation in laminar flows. Phys Rev E 2001;64:046307.
[2] Ben-Avraham D, Havlin S. Diffusion and reactions in fractals and disordered systems. Cambridge: Cambridge University Press; 2000.

[3] Brockmann D, Hufnagel L. Phys Rev Lett 2007;98:178301.
[4] Cencini M, Torcini A, Vergni D, Vulpiani A. Thin front propagation in steady and unsteady cellular flows. Phys Fluids 2003;15:679–88.
[5] Del-Castillo-Negrete D, Carreras BA, Lynch VE. Phys Rev Lett 2003;91:018302.
[6] Field RJ, Burger M. Oscillations and traveling waves in chemical systems. New York: Wiley; 1985.
[7] Fisher RA. Proc Annu Symp Eugen Soc 1937;7:355.
[8] Grindrod P. The theory and applications of reaction diffusion equations: patterns and waves. Oxford: Clarendon Press; 1996.
[9] Karolyi G, Pentek A, Toroczkai Z, Tel T, Grebogi C. Chemical or biological activity in open chaotic flows. Phys Rev E 1999;59:5468–81.
[10] Karolyi G, Pentek A, Scheuring I, Tel T, Toroczkai Z. Chaotic flow: The physics of species coexistence. Proc Nat Acad Sci USA 2000;97:13661–5.
[11] Kolmogorov AN, Petrovskii IG, Piskunov NS. Moscow Univ Math Bull (Engl Transl) 1937;1:1.
[12] Mancinelli R, Vergni D, Vulpiani A. Europhys Lett 2002;60:532.
[13] Marcus P. Numerical simulation of Jupiter's Great Red Spot. Nature 1988;331:693.
[14] Neufeld Z. Excitable media in a chaotic flow. Phys Rev Lett 2001;87:108301.
[15] Neufeld Z, Kiss IZ, Zhou C, Kurths J. Synchronization and oscillator death in oscillatory media with stirring. Phys Rev Lett 2003;90:084101.
[16] Nugent CR, Quarles WM, Solomon TH. Experimental studies of pattern formation in a reaction–advection–diffusion system. Phys Rev Lett 2004;93:218301.
[17] Paoletti MS, Solomon TH. Experimental studies of front propagation and mode-locking in an advection–reaction–diffusion system. Europhys Lett 2005;69:819–25.
[18] Paoletti MS, Solomon TH. Front propagation and mode-locking in an advection–reaction–diffusion system. Phys Rev E 2005;72:046204.
[19] Paoletti MS, Nugent CR, Solomon TH. Synchronization of oscillating reactions in an extended fluid system. Phys Rev Lett 2006;96:124101.
[20] Schwartz ME, Solomon TH. Chemical reaction fronts in ordered and disordered cellular flows with opposing winds. Phys Rev Lett 2008;100:028302.
[21] Sommeria J, Meyers SD, Swinney HL. Laboratory simulation of Jupiter's Great Red Spot. Nature 1988;331:689.
[22] Tel T, de Moura A, Grebogi C, Karolyi G. Chemical and biological activity in open flows: a dynamical system approach. Phys Rep 2005;413:91–196.